Research Square

Preprints are preliminary reports that have not undergone peer review.
They should not be considered conclusive, used to inform clinical practice,
or referenced by the media as validated information.

Rice husk pretreatment alters fermentable sugar production, aromatic compound profiles, and n-butyric acid fermentation

Hyojung Park
Korea Institute of Ceramic Engineering and Technology
Jong In Won
Korea Institute of Ceramic Engineering and Technology
Jin Hyung Lee
Korea Institute of Ceramic Engineering and Technology
Byoung Seung Jeon
a1trust@kicet.re.kr

Korea Institute of Ceramic Engineering and Technology

Research Article

Keywords: rice husk, n-butyric acid, Clostridium tyrobutyricum, pretreatment, hydrolysate composition, GC×GC-TOFMS

Posted Date: November 11th, 2026

DOI: https://doi.org/10.21203/rs.3.rs-11410889/v1

License: This work is licensed under a Creative Commons Attribution 4.0 International License.
Read Full License

Abstract

Rice husk hydrolysates produced using different pretreatment methods can exhibit different fermentation responses even after adjusting the fermentable sugar concentration to the same level. In this study, dilute-acid, alkaline, ethanol-organosolv, and ball-milling pretreatments were compared for sugar production and subsequent *n*-butyric acid fermentation by *Clostridium tyrobutyricum* BAS7. After enzymatic hydrolysis, each hydrolysate was concentrated to 60 g/L total glucose and xylose without adding commercial sugars. The dilute-acid and alkaline hydrolysates produced 26.45 and 26.52 g/L *n*-butyric acid, respectively, both of which were significantly higher than that of the commercial-glucose control. The alkaline hydrolysate showed a numerically lower maximum cell growth (OD600 6.81) and significantly lower fermentation gas formation (20.00 mL/mL) than the control (OD600 10.78 and 23.23 mL/mL), although the difference in maximum cell growth was not significant after Dunnett's adjustment. GC×GC-TOFMS profiling showed pretreatment-dependent differences in aromatic-compound profiles, with the alkaline hydrolysate exhibiting the highest relative signal for carboxyl-containing aromatic compounds. Veratric acid supplementation showed a concentration-dependent numerical decrease in fermentation gas formation; however, the differences from the control were not statistically significant. These findings indicate that pretreatment-dependent hydrolysate composition, in addition to fermentable sugar concentration, was associated with downstream fermentation performance.

1. Introduction

In lignocellulosic bioconversion, pretreatment is an essential step for improving subsequent enzymatic saccharification and microbial fermentation by reducing biomass recalcitrance and increasing enzyme accessibility to carbohydrate polymers [1, 2]. Common pretreatment methods include physical (e.g., ball milling), physicochemical [3], and chemical (e.g., organosolv, acid, and alkaline) approaches, all of which differ in their deconstruction mechanisms, sugar recovery, and formation of soluble byproducts that can impact subsequent fermentation [2, 4].

A major disadvantage of several pretreatments is the generation of degradation products that may inhibit microbial activity. These common byproducts form under unfavorable alkaline and acidic conditions and include phenolic compounds arising from carbohydrate and lignin degradation, aldehydes, and organic acids [5–8]. The presence of these byproducts during fermentation may affect microbial growth, hampering the productivity and yields of target compounds [9, 10]. Molecular dynamics and experimental assays conducted by Vermaas et al. (2019) revealed that lignin-derived phenolic compounds may permeate microbial membranes through passive diffusion. Sui et al. (2025) found that membrane fluidity and permeability may be disrupted by potential hydrophobic interactions between phenolics and lipid bilayers [11]. Nevertheless, the nonsugar fraction of lignocellulosic hydrolysates contains numerous low-abundance compounds with diverse chemical properties, and targeted high-performance liquid chromatography (HPLC) or conventional gas chromatography (GC) methods may not adequately delineate this chemical complexity. Therefore, nontargeted metabolomics is used to detect and prioritize potential fermentation inhibitors in lignocellulosic hydrolysates [12].

Hence, characterizing these inhibitors remains challenging, complicating downstream separation processes and restricting the complete exploitation of enzymatic hydrolysates [13–15]. Although numerous studies have compared pretreatment methods with the aim of minimizing solid loss and maximizing sugar yields [16–18], relatively few have explored the formation of inhibitory compounds during pretreatment and their functional effects on microbial bioproduction.

Biomass-derived hydrolysates can also exhibit fermentation behavior different from that of media prepared with purified sugars. For instance, Kwon et al. (2016) reported that *Clostridium beijerinckii* cultivated with a planetary-milled *Pinus rigida* hydrolysate generated slightly more butanol and higher amounts of organic acids than cultures supplied with the same glucose concentration [2], In another study, corn-stover hydrolysate containing soluble phenolic compounds did not inhibit the growth of *Saccharomyces cerevisiae* compared with an artificial glucose medium [19]. These data indicate that the effect of a lignocellulosic hydrolysate cannot be determined only from its sugar concentration or the presence of individual inhibitory compounds.

Previous studies have also demonstrated that *C. tyrobutyricum* can utilize lignocellulosic hydrolysates; however, the fermentation response depends strongly on the biomass source and hydrolysate composition. Liu et al. (2013) reported butyrate yields of approximately 0.42–0.46 g/g glucose from several dilute-acid lignocellulosic hydrolysates and observed growth inhibition with some hydrolysates [20]. Wei et al. (2013) obtained butyrate yields of 0.45–0.54 g/g sugar from sugarcane bagasse hydrolysate without detoxification [21]. Furthermore, phenolic compounds and furan derivatives present in biomass hydrolysates inhibit the growth and productivity of *C. tyrobutyricum* [22]. Nevertheless, most previous studies focused on hydrolysate tolerance, detoxification, or overall fermentation performance. The relationship between pretreatment-dependent non-sugar composition and fermentation behavior under a normalized fermentable-sugar concentration has received less attention.

Rice husk is an abundant agricultural byproduct produced during rice milling. It is considered a promising and sustainable feedstock for biorefinery applications [23]. Various physicochemical pretreatment approaches can be applied to rice husk to enhance its enzymatic hydrolysis efficiency. In this study, enzymatic hydrolysates were prepared from rice husk subjected to four pretreatment methods, viz., ball milling, ethanol-based organosolv, dilute acid hydrolysis (hereafter referred to as dilute acid), and alkaline treatment with NaOH. These methods were selected to represent distinct mechanisms of lignocellulosic deconstruction and to enable comparison their effects on enzymatic digestibility and the aromatic-compound formation. Ball milling disrupts biomass structure through mechanical shear, resulting in limited formation of soluble degradation products [2]. Pretreatment with ethanol organosolv induces α-ethoxylation reactions in lignin, a process facilitated by acetic acid released during acetyl group hydrolysis, and affects β-O-4 linkages [24, 25]. The present study characterized pretreatment-dependent non-sugar profile, investigated the effect of selected aromatic compounds on *n*-butyric acid fermentation, and evaluated fermentable-sugar production. A valuable biobased chemical, *n*-butyric acid, is used in various industrial applications, such as pharmaceuticals, food additives, cosmetics, textiles, and disinfectants. It is also a key material in the production of textile

auxiliaries, plastics, surfactants, and plasticizers [26]. *Clostridium tyrobutyricum* BAS7 is used for bioconversion for its ability to produce *n*-butyric acid, hydrogen, acetic acid, and carbon dioxide. It is highly efficient in anaerobic metabolism and is thus suitable as a model bacterium for investigating fermentation performance under different hydrolysate compositions [27, 28]. The hydrolysates were analyzed by comprehensive two-dimensional gas chromatography–time-of-flight mass spectrometry (GC×GC-TOFMS) to compare pretreatment-dependent nonsugar profiles. *C. tyrobutyricum* BAS7 was then used to produce *n*-butyric acid from the concentrated hydrolysates. Changes in byproduct profiles resulting from microbial metabolism were evaluated by comparing hydrolysate composition before and after fermentation. The study focused on the association between pretreatment-dependent hydrolysate composition and differences in cell growth, fermentation gas formation, and *n*-butyric acid production.

2. Materials and methods

2.1 Materials

Rice husk was collected from a rice processing facility located in Ochang, Chungbuk Province, Republic of Korea. The rice husk biomass was harvested in 2021, air-dried at room temperature, and used directly in pretreatment. CH_3COOH (99.5%), H_2SO_4 (70%), and NaOH powder (98%) were purchased from Samchun Chemicals Inc. (Seoul, Republic of Korea). Before use, NaOH was dissolved in distilled water, whereas the other chemicals were used as received. Cellulose cocktail (Cellic® CTec3) was purchased from Novozyme Co. (Bagsvaerd, Denmark).

2.2 Pretreatment and enzymatic hydrolysis

The pretreatment methods used in this study were adapted from previously reported protocols with slight modifications to the reaction conditions. Rice husk was used at a solid loading of 10% (w/v) for chemical pretreatments (dilute acid, alkaline, and organosolv), corresponding to 10 g of biomass per 100 mL of solution. For ball milling, 7.2 g of rice husk was used. For pretreatment with dilute acid, rice husk was treated with H_2SO_4 (2%, *v/v*) at 130°C (3 h) [29]. For alkaline pretreatment, rice husk was immersed in NaOH solution (4%, *w/v*) and incubated at 130°C (6 h) [30]. For organosolv pretreatment, rice husk was treated with ethanol (50%, *v/v*) at 170°C (1 h) [31]. Ball milling was performed using a Pulverisette 5 Planetary Mill (Fritsch, Idar-Oberstein, Germany) [31]. Rice husk was placed in a jar and mixed with 50 mM sodium acetate buffer (pH 4.8) to fill 35% of the jar volume. Steel balls measuring 10 mm in diameter were added to the jar at a biomass-to-ball volume ratio of 1:1. The solid-to-liquid ratio was maintained at 5% (*w/v*), and milling was performed at 300 rpm (1 h). After the chemical pretreatments, the solid fractions were recovered by filtration using a 0.2-μm filter paper and repeatedly washed with deionized water to remove residual chemicals until the pH of the wash effluent reached 7.0. The ball-milled biomass was recovered separately after physical pretreatment and used for subsequent analysis without the neutralization washing step applied to the chemically pretreated samples.

Enzymatic hydrolysis was performed at pH 4.8 in the presence of a 50-mM sodium acetate buffer. To achieve a final enzyme loading of 15 filter paper units (FPU)/g biomass, Cellic® CTec3 (a multienzyme complex containing cellulases, hemicellulases, and high levels of β-glucosidase) was added to the pretreated biomass. The solid-to-liquid ratio was maintained at 5% (*w/v*). Enzymatic hydrolysis was performed at 50°C for 72 h with shaking at 200 rpm using a rotator (JEIO TECH, Daejeon, Republic of Korea), after which the obtained hydrolysate was concentrated using a centrifugal evaporator (CVE-3000, EYELA, Tokyo, Japan) operating at 1.3 kPa and at 30°C. Each hydrolysate was concentrated until the combined concentration of glucose and xylose reached 60 g/L. No commercial glucose or xylose was added during this step.

2.3 Fermentation conditions

C. tyrobutyricum BAS7 was cultured in modified P2 basal medium at 37°C and pH 6.5. Fermentation was performed in 200-mL serum bottles with a working volume of 40 mL, and the cultures were incubated with shaking at 150 rpm. To establish anaerobic conditions, high-purity nitrogen gas (99.999%) was directly bubbled through the medium for 30 min using a 23-gauge needle. The serum bottles were then sealed with aluminum caps and sterilized by autoclaving.

The modified P2 basal medium contained 0.5 g/L KH_2PO_4, 0.5 g/L K_2HPO_4, 1.7 g/L CH_3COOH, 0.2 g/L $MgSO_4{\cdot}7H_2O$, 0.01 g/L $MnSO_4{\cdot}7H_2O$, 0.01 g/L $FeSO_4{\cdot}7H_2O$, 0.01 g/L NaCl, 0.001 g/L *p*-aminobenzoic acid, 0.001 g/L thiamine, 0.00001 g/L biotin, 15.014 g/L calcium carbonate, and 5 g/L yeast extract [31]. For the commercial glucose control, 60 g/L glucose was used as the carbon source.

For hydrolysate-based fermentation, the carbon source was supplied by the concentrated hydrolysate itself. The combined concentration of glucose and xylose was adjusted to 60 g/L by concentrating each hydrolysate, whereas the glucose-to-xylose composition depended on the pretreatment method. No commercial sugars were added to the hydrolysate media.

2.4 Analytical methods

Using standard protocols established by the National Renewable Energy Laboratory (NREL-LAP, 2008), the ash, lignin, and carbohydrate contents of the rice husk biomass were quantified by two-step acid hydrolysis to separate sugars from cellulose and hemicellulose.

Sugar composition was evaluated by HPLC using a refractive index detector (Waters Alliance e2695/2414 RI detector; Agilent 1,260 Infinity II; Waters Co., Milford, MA, USA; Agilent Technologies, Santa Clara, CA, USA). A Hi-Plex H USP L17 column (Agilent Technologies, Santa Clara, CA, USA) was used and maintained at 70°C. Degassed distilled water was used as the mobile phase at a flow rate of 0.5 mL/min.

Acid-soluble lignin was estimated quantitatively at 320 nm using UV spectrophotometry (V-550 UV/VIS, Jasco, Hachioji, Japan), whereas acid-insoluble lignin was quantified by combustion at 575°C using a

muffle furnace (M-25P, Hantech, Gunpo, Republic of Korea) (Kline et al., 2010). All measurements were performed in triplicate to ensure statistical robustness.

After dilution with NaOH (0.1 N), microbial growth was monitored by measuring the optical density at 600 nm using a UV/Vis spectrophotometer (X-ma 1,000, Human Corporation, Seoul, Republic of Korea). pH was measured using a HI2550 pH meter equipped with a HI1330 pH probe (Hanna Instruments, Padova, Italy).

n-Butyric acid, glucose, xylose, and acetic acid concentrations in the fermentation broth were quantified using an HPLC system equipped with a refractive index detector (Waters Alliance e2695/2414 Refractive Index Detector, Waters Co., Milford, MA, USA). A Hi-Plex H USP L17 column (7.7 × 100 mm, 8 µm, Agilent Technologies, Santa Clara, CA, USA) was used with H_2SO_4 (0.0085 M) as the mobile phase. Isocratic elution was conducted at a flow rate of 0.6 mL/min, and both the column and detector temperatures were maintained at 40°C. Analyses were conducted in triplicate.

The apparent *n*-butyric acid yield based on measured monosaccharide consumption was calculated as the amount of *n*-butyric acid produced divided by the amount of glucose and xylose consumed. This value was used for comparison among the fermentation conditions. It was not considered a complete carbon-based stoichiometric yield because other carbon-containing components in the hydrolysates and medium were not included in the calculation.

Metabolite profiling was performed using a GC×GC-TOFMS system (LECO Corporation, St. Joseph, MI, USA) on an Agilent 8890 GC system (Agilent Technologies, Palo Alto, CA, USA) equipped with a split/split less injector. The primary column was DB-5MS UI (30 m × 0.24 mm × 0.25 µm), whereas the secondary column was Rxi-17Sil MS (0.76 m × 0.25 mm × 0.25 µm). The front inlet was maintained at 250°C with a carrier gas flow rate of 1 mL/min. The oven temperature was programmed to increase from 40°C (held for 2.2 min) to 300°C (held for 5 min) at 6°C/min. For GC×GC-TOFMS sample preparation, the metabolites were extracted with an equal volume of ethyl acetate, and pH was adjusted to ≤ 2 using HCl (1 N). The ethyl acetate layer was concentrated and dried using a centrifugal evaporator (CVE-3000, EYELA, Tokyo, Japan). Methoxyamine hydrochloride (10 µL) containing 20 mg/mL pyridine was added to the dried extract and incubated with shaking at 30°C at 1000 rpm (90 min) for derivatization. Then, 90 µL N-methyl-N-(trimethylsilyl)trifluoroacetamide was added and incubated at 37°C (30 min). Samples (1 µL each) were injected with a split at a ratio of 1:20.

Data were collected and processed using the ChromaTOF software (v5.55.29.0, LECO, St. Joseph, MI, USA). Deconvoluted peak apexes (components) were automatically detected, and tentative compound annotations were assigned by matching EI mass spectra against the NIST Mainlib and Replib libraries using a spectral similarity threshold of 800.

Peak areas were used for relative comparison among samples. Because calibration curves and internal standards were not used for all annotated compounds, the peak-area data were not converted into absolute concentrations.

2.5 Statistical analysis

All fermentation experiments were initially conducted in triplicate (n = 3). In the pretreatment-comparison experiment, one control replicate was excluded from the statistical analysis because of a cultivation failure, resulting in n = 2 for the control and n = 3 for each pretreatment condition. All groups in the aromatic-compound supplementation experiment were analyzed in triplicate (n = 3). Data are presented as the mean ± standard deviation. Differences in sugar consumption, maximum cell growth, fermentation gas volume, final pH, *n*-butyric acid concentration, and apparent *n*-butyric acid yield were evaluated using one-way analysis of variance (ANOVA), followed by Dunnett's multiple comparison test to compare each treatment with the corresponding control. Adjusted *p*-values < 0.05 were considered statistically significant. Principal component analysis (PCA) was performed using GraphPad Prism 8.0 (GraphPad Software, Boston, MA, USA). The variable included maximum cell growth, glucose, xylose, and summed TIC peak areas of carboxyl-containing and non-carboxylated aromatic features. Data were mean-centered and autoscaled before PCA. PCA was used as an exploratory analysis and was not used for statistical inference.

3. Results and Discussion

3.1 Production of fermentable sugars from rice husks subjected to different pretreatment methods

Raw rice husk contained (wt%) ash (12.88%), cellulose (34.61%), hemicellulose (18.23%), and lignin (29.64%). Rice husk contains a higher ash content than several other lignocellulosic biomasses, and its complex structural composition can hinder enzyme access to cellulose, thereby hindering hydrolysis [32]. Therefore, rice husk was pretreated to enhance the production of fermentable sugars. In this study, the pretreatments were dilute acid, alkali, organosolv, and ball milling. As a control, enzymatic hydrolysis of untreated rice husk produced only 0.67 g/L glucose (data not shown), which was probably due to its high ash and lignin contents. Nevertheless, pretreatment markedly increased fermentable-sugar concentrations. The alkaline treatment produced the highest glucose concentration after enzymatic hydrolysis (28.69 g/L), followed by ball milling (20.13 g/L), dilute acid (11.07 g/L), and organosolv pretreatment (10.81 g/L) (Table 1). Moreover, xylose concentrations of 8.17 and 4.98 g/L were detected after alkaline and ball milling pretreatments, respectively. The observed variations in sugar composition and concentration were attributed to the distinct mechanisms of action of each pretreatment method, which probably affected subsequent microbial fermentation.

Table 1
Glucose and xylose concentration in enzymatic hydrolysates before concentration for fermentation (g/L)

Glucose	Dilute acid	Alkaline	Organosolv	Ball milling
	11.07 ± 0.15	**28.69 ± 0.35**	**10.81 ± 3.25**	**20.13 ± 0.1**
Xylose	0	8.17 ± 0.12	0	4.98 ± 0.12

The hydrolysates differed in both sugar composition and the degree of concentration required to reach 60 g/L total monosaccharides for fermentation. Therefore, the final fermentation media could also differ in nonsugar components derived from the respective pretreatment processes.

Based on the sugar concentration before the concentration step, the approximate concentration factors required to reach 60 g/L total glucose and xylose were 5.42 for dilute acid, 1.63 for alkaline, 5.55 for organosolv, and 2.39 for ball milling. Hence, the final nonsugar composition of the fermentation media could reflect both pretreatment chemistry and the different concentration factors used during medium preparation. Nevertheless, the alkaline hydrolysate required the lowest concentration factor and later exhibited the highest GC×GC-TOFMS signal for carboxyl-containing aromatic compounds. Therefore, the high aromatic signal in the alkaline hydrolysate cannot be explained only by the concentration step. Alkaline pretreatment disrupts lignin–carbohydrate linkages and promotes lignin solubilization [33], which provides a plausible chemical basis for the distinct aromatic profile observed in this study. A recent study by Dong et al. (2026) also demonstrated that NaOH pretreatment of rice husk changed hydrolysable sugar composition and markedly altered downstream fermentative hydrogen production [34]. These data support the importance of investigating pretreatment performance beyond sugar concentration alone.

3.2 Cultivation of C. tyrobutyricum using saccharification hydrolysates

After enzymatic hydrolysis, each hydrolysate was concentrated to 60 g/L total glucose and xylose and used for fermentation without detoxification or further purification. No commercial sugar was added to the hydrolysate media. Therefore, the total measured monosaccharide concentration was similar among the hydrolysate conditions, although the glucose-to-xylose composition differed according to the pretreatment method.

Cell growth and sugar consumption differed among the hydrolysate conditions (Fig. 1a and Table 2). The organosolv hydrolysate exhibited the highest numerical maximum cell growth (OD600 13.06), although the difference from the commercial-glucose control (OD600 10.78) was not statistically significant (adjusted $p = 0.324$). The dilute-acid hydrolysate also showed no significant difference in maximum cell growth from the control. Conversely, the ball-milled hydrolysate demonstrated significantly lower maximum cell growth (OD600 5.19; adjusted $p < 0.01$). The alkaline hydrolysate also exhibited lower numerical maximum cell growth (OD600 6.81); however, the difference did not reach statistical

significance after Dunnett's adjustment (adjusted $p = 0.0524$). These growth differences cannot be attributed to a single component because the hydrolysates differed in both sugar composition and nonsugar composition. Sugar consumption also differed significantly from the control in all hydrolysate conditions. Compared with the control (54.80 ± 0.99 g/L), the amount of consumed monosaccharides was lower in the organosolv (45.20 ± 0.72 g/L), dilute-acid (42.30 ± 0.34 g/L), and ball-milled (51.52 ± 0.37 g/L) conditions, whereas the alkaline hydrolysate exhibited higher sugar consumption despite its lower numerical cell growth, indicating that substrate utilization was not directly proportional to biomass formation.

Table 2
Fermentation results of *C. tyrobutyricum* BAS7 under different pretreatment conditions

Type of pretreatment	**Consumed sugars (g/L)**	**Max. cell growth**	**Fermentation gas volume (mL/mL)**	**Final pH**	**Produced *n*-butyric acid (g/L)**	**Apparent *n*-butyric acid yield based on consumed monosaccharides (g/g)**
Control	54.80 ± 0.99	10.78 ± 0.88	23.23 ± 1.28	5.28 ± 0.01	24.08 ± 0.29	0.440 ± 0.010
Organosolv	45.20 ± 0.72	13.06 ± 0.88	22.73 ± 0.72	5.56 ± 0.06	24.82 ± 1.22	0.549 ± 0.028
Dilute acid	42.30 ± 0.34	11.01 ± 2.19	21.73 ± 1.03	5.46 ± 0.02	26.45 ± 0.45	0.624 ± 0.012
Alkaline	57.18 ± 0.95	6.81 ± 1.62	20.00 ± 0.68	5.78 ± 0.00	26.52 ± 0.44	0.463 ± 0.011
Ball milling	51.52 ± 0.37	5.19 ± 1.33	20.97 ± 1.15	5.67 ± 0.02	20.77 ± 0.70	0.404 ± 0.014

A lag phase was found in the dilute-acid, organosolv, and ball-milled conditions (Fig. 1a). Xylose was detected in the alkaline and ball-milled hydrolysates but not in the dilute-acid and organosolv hydrolysates. Nevertheless, the lower numerical cell growth observed in the alkaline and ball-milled conditions cannot be attributed solely to xylose because glucose remained the major sugar in both media. Furthermore, only the ball-milled condition exhibited a statistically significant reduction in maximum cell growth compared with the control. Therefore, the observed differences were considered to reflect the combined effects of sugar composition and other hydrolysate-derived components.

During the first 49 h, *n*-butyric acid accumulated earlier in the alkaline hydrolysate than in the other hydrolysate conditions (Fig. 1d). Compared with the commercial-glucose control, the alkaline hydrolysate demonstrated significantly lower fermentation gas production (20.00 ± 0.68 vs. 23.23 ± 1.28 mL/mL; adjusted $p < 0.05$) but significantly higher final *n*-butyric acid production (26.52 ± 0.44 vs. 24.08

± 0.29 g/L; adjusted $p < 0.05$). Sugar consumption was also significantly higher in the alkaline condition, whereas the reduction in maximum cell growth did not reach statistical significance after Dunnett's adjustment. Hence, sugar consumption, biomass formation, fermentation gas production, and *n*-butyric acid production did not change proportionally in the alkaline hydrolysate. This result indicates that total monosaccharide concentration alone did not explain the fermentation performance.

A similar difference between biomass hydrolysates and purified glucose media was observed in our previous study. Kwon et al. (2016) compared a planetary-milled *P. rigida* hydrolysate with a control containing the same glucose concentration and found slightly higher butanol production together with increased acetate and butyrate production in the hydrolysate culture. The hydrolysate also contained cellobiose and xylose in addition to glucose. These results indicate that fermentation performance in biomass hydrolysates cannot always be determined only from measured glucose consumption.

The fermentation data also demonstrated that maximum cell growth and *n*-butyric acid production were not directly coupled across the hydrolysates. The organosolv hydrolysate exhibited the highest maximum cell growth (OD600 13.06), although it was not significantly different from that in the control, and produced 24.82 g/L *n*-butyric acid. Conversely, the alkaline hydrolysate demonstrated lower maximum cell growth (OD600 6.81) but produced 26.52 g/L *n*-butyric acid and consumed 57.18 g/L measured sugars. The ball-milled hydrolysate also exhibited significantly lower maximum cell growth (OD600 5.19) and significantly lower final *n*-butyric acid production (20.77 g/L) than the control. In contrast, the alkaline hydrolysate exhibited significantly lower fermentation gas formation together with significantly higher *n*-butyric acid production. Therefore, reduced biomass formation alone did not predict *n*-butyric acid production. The different responses of the alkaline and ball-milled hydrolysates indicate that hydrolysate composition affected carbon utilization and product formation in a pretreatment-dependent manner.

Previous studies using *C. tyrobutyricum* also reported substantial differences among lignocellulosic hydrolysates. For instance, Liu et al. (2013) obtained butyrate yields of 0.42–0.46 g/g glucose from dilute-acid hydrolysates of wheat straw and switchgrass, whereas a corn-stover hydrolysate caused marked growth inhibition [20]. Wei et al. (2013) reported butyrate yields of 0.45–0.54 g/g sugar from sugarcane bagasse hydrolysate without detoxification [21]. Suo et al. further demonstrated that hydrolysate-derived phenolics and furan derivatives can reduce *C. tyrobutyricum* growth and productivity [22]. Combined with the present results, these studies indicate that lignocellulosic hydrolysates should not be considered equivalent fermentation substrates solely because their fermentable-sugar concentrations are similar.

The dilute-acid hydrolysate produced 26.45 g/L *n*-butyric acid, whereas only 42.30 g/L measured glucose and xylose were consumed, resulting in an apparent yield of 0.624 ± 0.012 g/g. Both the final *n*-butyric acid concentration (adjusted $p < 0.05$) and apparent yield (adjusted $p < 0.0001$) were significantly higher than those of the commercial-glucose control. However, the apparent yield was higher than the theoretical mass yield anticipated from glucose alone and hence cannot be interpreted as a complete

stoichiometric yield. In addition to unquantified carbon-containing compounds in the hydrolysate, the modified P2 medium contained 1.7 g/L acetate. *C. tyrobutyricum* has been reported to produce butyrate through a butyryl-CoA/acetate CoA-transferase route that can involve acetate reassimilation [35]. Therefore, carbon derived from medium acetate may also contribute to the apparent sugar-based yield. Hence, the present yield values should therefore be used only for comparison among the tested media and not as complete carbon-balance yields.

Fermentation gas formation should also be interpreted cautiously. The alkaline hydrolysate showed lower total fermentation gas (20.00 mL/mL) than the commercial-glucose control (23.23 mL/mL); however, the gas composition was not measured. In addition, 15.014 g/L $CaCO_3$ was present in the medium, and CO_2 can be released during acid neutralization. Therefore, total fermentation gas was treated as a process response rather than as a direct measure of hydrogen formation or electron disposal.

3.3 Enzymatic hydrolysate profiling during fermentation

As described in Section 3.2, the alkaline hydrolysate demonstrated early accumulation of *n*-butyric acid despite relatively low cell growth. To examine whether the hydrolysates differed in their nonsugar composition, initial and postfermentation samples were profiled using GC × GC-TOFMS.

Total ion chromatogram (TIC) feature counts are summarized in Table 3. The initial organosolv and dilute-acid samples contained 4,247 and 4,305 detected features, respectively, which decreased to 1,303 and 1,373 after fermentation (Fig. S1 and Fig. S2). The ball-milled sample had the highest initial feature count (5,441), which decreased to 1,063, whereas the alkaline sample showed a decrease in feature count from 3,811 to 1,200. Across all conditions, several features were no longer detected after fermentation. This change may reflect biological conversion, adsorption, or physicochemical change in compound partitioning and solubility. However, the ethyl-acetate blank also contained a substantial number of detected features (1,682 before and 955 after processing). For this reason, feature count was used only as a descriptive index of chromatographic complexity and was not interpreted as compound concentration or inhibitor load.

Table 3
Changes in detected GC×GC-TOFMS feature counts before and after fermentation

Pretreatment conditions	Detected features		Matched/unique feature		Unique peaks in only before sample	Unique peaks in only after sample	Common peaks between before & after
	Before	After	Before	After			
Organosolv	4,247	1,303	62	30	160	59	15
Dilute acid	4,305	1,373	62	23	164	59	16
Alkaline	3,811	1,200	63	17	151	52	12
Ball milling	5,441	1,063	46	22	169	41	7
Control	_*	1,160	_*	23	_*	_*	_*
Ethyl acetate	1,682	955	167	92	_*	_*	_*

Total peaks represent all detected GC×GC-TOFMS features within a given sample. Unique peaks refer to features detected only in a particular sample. Features present only before or after fermentation are reported separately, whereas common peaks refer to features detected in both prefermentation and postfermentation samples. Feature counts were used only as descriptive measures of chromatographic complexity and were not interpreted as compound concentrations or inhibitor load.

Carboxyl-containing and non-carboxylated aromatic features were grouped according to their tentative compound annotations, and their summed TIC peak areas were compared semi-quantitatively (Table S1). The alkaline hydrolysate demonstrated the highest summed TIC peak area for carboxyl-containing aromatic compounds, followed by the dilute-acid and organosolv hydrolysates. The ball-milled hydrolysate exhibited the lowest summed signal for this group. These comparisons represent relative GC×GC-TOFMS signals and not absolute compound concentrations.

The relative distribution of aromatic compound classes also differed among pretreatments. When the summed signal of carboxyl-containing aromatic features was expressed relative to the total summed aromatic signal, the approximate proportions were 2.8% for organosolv, 3.0% for dilute acid, 11.1% for alkaline, and 1.2% for ball milling. Although these values are semi-quantitative and do not represent molar fractions, the alkaline hydrolysate was distinguished not only by a high absolute TIC signal for carboxyl-containing aromatic features but also by its higher relative contribution to the aromatic profile. Importantly, this pattern was observed despite the alkaline hydrolysate having the lowest concentration factor before fermentation, supporting the interpretation that the alkaline pretreatment chemistry itself contributed to the distinct aromatic profile.

PCA was used as an exploratory analysis to visualize the relative distribution of the four hydrolysates based on sugar composition, cell growth, and the summed TIC areas of selected aromatic-compound groups (Fig. 2). PC1 and PC2 accounted for 70.37% and 28.90% of the total variance, respectively. The alkaline hydrolysate was positioned in the same direction as carboxyl-containing aromatic features,

whereas the ball-milled hydrolysate exhibited a different overall profile. Because only four hydrolysate conditions were included, PCA was not used for statistical inference or causal interpretation.

3.4 Effect of selected aromatic carboxylic acids on n-butyric acid fermentation

Veratric acid, DL-atrolactic acid, and vanillactic acid were tentatively annotated among the carboxyl-containing aromatic compounds detected in the hydrolysates (Table S2). Because vanillactic acid was not commercially available, veratric and DL-atrolactic acids were selected for supplementation experiments. Three concentrations (100 μM, 1 mM, and 5 mM) were tested to examine their effects on glucose consumption, *n*-butyric acid production, fermentation gas formation, cell growth, and pH (Fig. 3 and Table 4). Because the native concentrations of these compounds in the hydrolysates were not determined, the supplementation concentrations were used to examine physiological responses and must not be interpreted as reconstruction of the actual hydrolysate exposure.

Table 4
Fermentation results of *C. tyrobutyricum* BAS7 under supplementation with selected aromatic carboxylic acids

Control	Consumed glucose (g/L)	Production gas volume (mL/mL)	Final pH	Produced *n*-butyric acid (g/L)	Apparent *n*-butyric acid yield based on consumed glucose (g/g)
	58.59 ± 0.75	**21.88 ± 0.85**	**5.10 ± 0.00**	**26.53 ± 0.28**	**0.453 ± 0.001**
100 μM Veratric acid	58.97 ± 2.28	20.32 ± 3.02	5.11 ± 0.03	27.00 ± 0.71	0.459 ± 0.027
1 mM Veratric acid	57.51 ± 0.37	19.90 ± 0.70	5.07 ± 0.06	26.84 ± 0.55	0.467 ± 0.012
5 mM Veratric acid	54.02 ± 1.70	18.00 ± 1.32	4.97 ± 0.01	24.61 ± 1.07	0.456 ± 0.058
100 μM DL-atrolactic acid	61.50 ± 1.11	18.85 ± 3.07	5.12 ± 0.02	26.02 ± 0.15	0.423 ± 0.007
1 mM DL-atrolactic acid	59.27 ± 0.87	17.17 ± 0.71	5.12 ± 0.05	25.74 ± 0.58	0.434 ± 0.011
5 mM DL-atrolactic acid	55.58 ± 0.15	19.59 ± 2.39	4.98 ± 0.01	23.52 ± 0.20	0.423 ± 0.004

At 100 μM and 1 mM, neither veratirc acid nor DL-atrolactic acid significantly affected the measured fermentation parameters compared with the control (Fig. 3 and Table 4). At 5 mM, veratric acid significantly reduced glucose consumption (adjusted $p < 0.01$), final pH (adjusted $p < 0.01$), and *n*-butyric acid production (adjusted $p < 0.05$). In contrast, 5 mM DL-atrolactic acid significantly decreased final pH (adjusted $p < 0.01$) and n-butyric acid production (adjusted $p < 0.001$), whereas the reduction in glucose consumption was not statistically significant. Apparent *n*-butyric acid yield was not significantly different from the control at any tested concentration of either compound.

Veratric acid showed a numerical concentration-dependent decrease in fermentation gas formation, with values of 20.32, 19.90, and 18.00 mL/mL at 100 μM, 1 mM, and 5 mM, respectively. These values corresponded to decreases of 7.1%, 9.0%, and 17.7% compared with those in the control. However, none of the veratric acid treatments showed a statistically significant difference in fermentation gas formation

after Dunnett's adjustment. DL-atrolactic acid also showed lower numerical fermentation gas formation than the control; however, none of the tested concentrations produced a statistically significant difference. Maximum cell growth was not significantly different from the control under any aromatic-acid supplementation condition.

Veratric acid exhibited a concentration-dependent numerical decrease in fermentation gas formation without a corresponding increase in *n*-butyric acid production. Because the decrease in fermentation gas formation was not statistically significant, the result should be considered a trend rather than a confirmed inhibitory effect on gas-forming metabolism. Nevertheless, the supplementation experiment did not reproduce the overall fermentation response observed with the alkaline hydrolysate. Previous studies have demonstrated that lignin-related aromatic compounds can partition into and permeate biological membranes [36], and phenolic stress in *C. tyrobutyricum* can alter the expression of genes associated with phenolic reduction, heat-shock response, and membrane transport [37]. Moreover, lignin-derived phenolics change fermentation-product distributions in *C. acetobutylicum* [38]. These findings support the possibility that aromatic compounds can affect cellular physiology through more than simple growth inhibition.

n-Butyric acid synthesis in *C. tyrobutyricum* is also coupled to cellular redox and hydrogen metabolism. Feng et al. demonstrated that perturbation of hydrogenase HydA increased the intracellular NADH/NAD^+ ratio, decreased acetate accumulation, and increased butyrate yield [39]. Moreover, some polyphenolic compounds function as redox mediators or electron shuttles under appropriate electrochemical conditions [40]. This provides a relevant metabolic context for considering the numerical decrease in fermentation gas formation observed after veratric acid supplementation. Nevertheless, the present study did not measure H_2 and CO_2 separately, intracellular NADH/NAD^+, ferredoxin, ATP, membrane potential, or hydrogenase activity. Furthermore, a portion of the measured gas could originate from CO_2 released during $CaCO_3$-mediated neutralization. Therefore, a change in redox allocation is compatible with the observed response but is not demonstrated by the present data. The redox-related interpretation should therefore be regarded as a working hypothesis (Fig. 4).

The single-compound supplementation experiments also demonstrated that the alkaline-hydrolysate phenotype could not be attributed to veratric acid alone. This difference was also evident statistically, wherein the alkaline hydrolysate exhibited significantly lower fermentation gas formation together with significantly higher *n*-butyric acid production than the control, whereas veratric acid did not significantly reduce fermentation gas formation at any tested concentration and significantly decreased *n*-butyric acid production at 5 mM. The alkaline hydrolysate contained a distinct mixture of carboxyl-containing aromatic features together with glucose and xylose, whereas the other hydrolysates differed in both sugar composition and nonsugar profile. Therefore, the fermentation response likely reflects the combined influence of multiple hydrolysate-derived components rather than one dominant compound. This interpretation is consistent with previous studies demonstrating that lignocellulosic hydrolysates can produce fermentation behaviors that differ from those of purified-sugar media [2, 19] and that *C.*

tyrobutyricum responds differently to different hydrolysate-derived inhibitors [22, 37]. The present data do not establish synergistic interactions among these compounds; however, they indicate the need to consider whole-hydrolysate composition when investigating downstream fermentation performance.

4. Conclusion

This study compared four rice husk pretreatment methods based on sugar production, hydrolysate composition, and subsequent *n*-butyric acid fermentation by *C. tyrobutyricum* BAS7. Although the total glucose and xylose concentration was adjusted to 60 g/L for all hydrolysate media, the fermentation responses differed depending on the pretreatment method. The dilute-acid and alkaline hydrolysates produced final *n*-butyric acid concentrations of 26.45 and 26.52 g/L, respectively, both of which were significantly higher than that of the commercial-glucose control. The alkaline hydrolysate also demonstrated significantly lower fermentation gas formation, whereas its lower maximum cell growth did not remain statistically significant after Dunnett's adjustment. GC×GC-TOFMS profiling revealed that the alkaline hydrolysate had a distinct aromatic-compound profile, including the highest relative contribution of carboxyl-containing aromatic features. Veratric acid supplementation resulted in a concentration-dependent numerical decrease in fermentation gas formation; however, this trend was not statistically significant and did not reproduce the overall response observed with the alkaline hydrolysate. These findings indicate that pretreatment selection should consider not only fermentable-sugar production but also the nonsugar composition of the resulting hydrolysate. The physiological mechanisms underlying the observed responses remain to be verified.

Declarations

Ethics approval and consent to participate

Not applicable. This study did not involve human participants or animals.

Consent for publication

Not applicable.

Competing interests

The authors declare that they have no competing interests.

Funding

This research was funded by the National Research Foundation of Korea (NRF) (grant 405 #2022M3A9F3082334).

Authors' contributions

H. Park.: Writing - original draft, investigation, Analysis. **J.I. Won.**: Investigation, Data analysis, Writing - original draft. **J.H. Lee**: Resources, Conceptualization, Writing - review & editing. **B.S.Jeon**: Conceptualization, Writing - review & editing.

Acknowledgements

Not applicable.

Availability of data and material

The datasets generated and/or analyzed during the current study are available from the corresponding author on reasonable request.

References

1. Wyman CE, Cai CM, Kumar R (2017) Bioethanol from lignocellulosic biomass. Encyclopedia of Sustainability Science and Technology. Springer, pp 1–27
2. Kwon JH, Kang H, Sang BI, Kim Y, Min J, Mitchell RJ, Lee JH (2016) Feasibility of a facile butanol bioproduction using planetary mill pretreatment. Bioresour Technol 199:283–287
3. Baksi S, Saha D, Saha S, Sarkar U, Basu D, Kuniyal J (2023) Pre-treatment of lignocellulosic biomass: review of various physico-chemical and biological methods influencing the extent of biomass depolymerization. Int J Environ Sci Technol 20(12):13895–13922
4. Kumar AK, Sharma S (2017) Recent updates on different methods of pretreatment of lignocellulosic feedstocks: a review. Bioresour Bioprocess 4(1):7
5. Adeboye PT, Bettiga M, Olsson L (2014) The chemical nature of phenolic compounds determines their toxicity and induces distinct physiological responses in *Saccharomyces cerevisiae* in lignocellulose hydrolysates. AMB Express 4(1):46
6. Luo H, Liu Z, Xie F, Bilal M, Peng F (2021) Lignocellulosic biomass to biobutanol: Toxic effects and response mechanism of the combined stress of lignin-derived phenolic acids and phenolic aldehydes to *Clostridium acetobutylicum*. Ind Crops Prod 170:113722
7. Østby H, Hansen LD, Horn SJ, Eijsink VG, Várnai A (2020) Enzymatic processing of lignocellulosic biomass: principles, recent advances and perspectives. J Ind Microbiol Biotechnol 47(9–10):623–657
8. Tang C, Gandla ML, Jönsson LJ (2023) LPMO-supported saccharification of biomass: effects of continuous aeration of reaction mixtures with variable fractions of water-insoluble solids and cellulolytic enzymes. Biotechnol Biofuels Bioprod 16(1):156

9. Kim Y, Kreke T, Hendrickson R, Parenti J, Ladisch MR (2013) Fractionation of cellulase and fermentation inhibitors from steam pretreated mixed hardwood. Bioresour Technol 135:30–38
10. Persson P, Andersson J, Gorton L, Larsson S, Nilvebrant NO, Jönsson LJ (2002) Effect of different forms of alkali treatment on specific fermentation inhibitors and on the fermentability of lignocellulose hydrolysates for production of fuel ethanol. J Agric Food Chem 50(19):5318–5325
11. Sui X, Guo L, Bao Z, Xian M, Zhao G (2025) Efflux pumps and porins enhance bacterial tolerance to phenolic compounds by inhibiting hydroxyl radical generation. Microorganisms 13(1):202
12. Zha Y, Westerhuis JA, Muilwijk B, Overkamp KM, Nijmeijer BM, Coulier L, Smilde AK, Punt PJ (2014) Identifying inhibitory compounds in lignocellulosic biomass hydrolysates using an exometabolomics approach. BMC Biotechnol 14(1):22
13. da Costa Lopes AM, Brenner M, Fale P, Roseiro LB, Bogel-Łukasik R (2016) Extraction and purification of phenolic compounds from lignocellulosic biomass assisted by ionic liquid, polymeric resins, and supercritical CO2. ACS Sustain Chem Eng 4(6):3357–3367
14. Freitas JV, Farinas CS (2017) Sugarcane bagasse fly ash as a no-cost adsorbent for removal of phenolic inhibitors and improvement of biomass saccharification. ACS Sustain Chem Eng 5(12):11727–11736
15. Lee SC, Park S (2016) Removal of furan and phenolic compounds from simulated biomass hydrolysates by batch adsorption and continuous fixed-bed column adsorption methods. Bioresour Technol 216:661–668
16. Eliana C, Jorge R, Juan P, Luis R (2014) Effects of the pretreatment method on enzymatic hydrolysis and ethanol fermentability of the cellulosic fraction from elephant grass. Fuel 118:41–47
17. Ruan L, Wu H, Wu S, Zhou L, Wu S, Shang C (2024) Optimizing the conditions of pretreatment and enzymatic hydrolysis of sugarcane bagasse for bioethanol production. ACS Omega 9(27):29566–29575
18. Taheri ME, Salimi E, Saragas K, Novakovic J, Barampouti EM, Mai S, Malamis D, Moustakas K, Loizidou M (2021) Effect of pretreatment techniques on enzymatic hydrolysis of food waste. Biomass Convers Biorefin 11(2):219–226
19. Gu Y, Byun H, Kim Y, Park D, Lee J (2019) Assessing the potential of facile biofuel production from corn stover using attrition mill treatment. Water-Energy Nexus 2:46–49
20. Liu S, Bischoff KM, Leathers TD, Qureshi N, Rich JO, Hughes SR (2013) Butyric acid from anaerobic fermentation of lignocellulosic biomass hydrolysates by *Clostridium tyrobutyricum* strain RPT-4213. Bioresour Technol 143:322–329
21. Wei D, Liu X, Yang ST (2013) Butyric acid production from sugarcane bagasse hydrolysate by *Clostridium tyrobutyricum* immobilized in a fibrous-bed bioreactor. Bioresour Technol 129:553–560
22. Suo Y, Fu H, Ren M, Yang X, Liao Z, Wang J (2018) Butyric acid production from lignocellulosic biomass hydrolysates by engineered *Clostridium tyrobutyricum* overexpressing Class I heat shock protein GroESL. Bioresour Technol 250:691–698

23. Park J, Gu Y, Park S, Hwang E, Sang B, Chun J, Lee J (2021) Two-stage continuous process for the extraction of silica from rice husk using attrition ball milling and alkaline leaching methods. Sustainability 13:7350
24. Guo Y, Zhou J, Wen J, Sun G, Sun Y (2015) Structural transformations of triploid of *Populus tomentosa* Carr. lignin during auto-catalyzed ethanol organosolv pretreatment. Ind Crops Prod 76:522–529
25. Wen JL, Xue BL, Sun SL, Sun RC (2013) Quantitative structural characterization and thermal properties of birch lignins after auto-catalyzed organosolv pretreatment and enzymatic hydrolysis. J Chem Technol Biotechnol 88(9):1663–1671
26. Diaz AB, Blandino A, Caro I (2018) Value added products from fermentation of sugars derived from agro-food residues. Trends Food Sci Technol 71:52–64
27. Qureshi N, Liu S, Saha BC (2022) Butyric acid production by fermentation: employing potential of the novel *Clostridium tyrobutyricum* strain NRRL 67062. Fermentation 8(10):491
28. Yu M, Zhang Y, Tang IC, Yang ST (2011) Metabolic engineering of *Clostridium tyrobutyricum* for n-butanol production. Metab Eng 13(4):373–382
29. Gutierrez S, Mangone F, Vergara P, Gonzalez V, Ferreira JP, Villar JC, Garcia-Ochoa F (2023) Lignocellulosic biomass pre-treatments by diluted sulfuric acid and ethanol-water mixture: A comparative techno-economic analysis. Bioresour Technol Rep 23:101514
30. Wang W, Wang X, Zhang Y, Yu Q, Tan X, Zhuang X, Yuan Z (2020) Effect of sodium hydroxide pretreatment on physicochemical changes and enzymatic hydrolysis of herbaceous and woody lignocelluloses. Ind Crops Prod 145:112145
31. Alvira P, Tomás-Pejó E, Ballesteros M, Negro MJ (2010) Pretreatment technologies for an efficient bioethanol production process based on enzymatic hydrolysis: a review. Bioresour Technol 101(13):4851–4861
32. Lau BB, Yeung T, Patterson RJ, Aldous L (2017) A cation study on rice husk biomass pretreatment with aqueous hydroxides: cellulose solubility does not correlate with improved enzymatic hydrolysis. ACS Sustain Chem Eng 5(6):5320–5329
33. Wang H, Chen Y, Yang Z, Deng H, Liu Y, Wei P, Zhu Z, Jiang L (2024) Metabolic and Bioprocess Engineering of *Clostridium tyrobutyricum* for Butyl Butyrate Production on Xylose and Shrimp Shell Waste. Foods 13(7):1009
34. Dong D, Zhao X, Lee JW (2026) Thermochemical pretreatment with ionic liquids for enhancing fermentative hydrogen production from rice husk. Biomass Bioenergy 207:108719
35. Lee J, Jang YS, Han MJ, Kim JY, Lee SY (2016) Deciphering *Clostridium tyrobutyricum* metabolism based on the whole-genome sequence and proteome analyses. mBio 7(3):e00743–e00716
36. Vermaas JV, Dixon RA, Chen F, Mansfield SD, Boerjan W, Ralph J, Crowley MF, Beckham GT (2019) Passive membrane transport of lignin-related compounds. Proc Natl Acad Sci USA 116(46):23117–23123

37. Luo L, Wei H, Kong D, Wan L, Jiang Y, Qin S, Suo Y (2024) Efficient production of Butyric acid from lignocellulosic biomass by revealing the mechanisms of *Clostridium tyrobutyricum* tolerance to phenolic inhibitors. Bioresour Technol 396:130427
38. Luo H, Zheng P, Xie F, Yang R, Liu L, Han S, Zhao Y, Bilal M (2019) Co-production of solvents and organic acids in butanol fermentation by *Clostridium acetobutylicum* in the presence of lignin-derived phenolics. RSC Adv 9(12):6919–6927
39. Feng J, Guo X, Cai F, Fu H, Wang J (2022) Model-based driving mechanism analysis for butyric acid production in *Clostridium tyrobutyricum*. Biotechnol Biofuels Bioprod 15(1):71
40. Hsueh CC, Wu CC, Chen BY (2019) Polyphenolic compounds as electron shuttles for sustainable energy utilization. Biotechnol Biofuels 12(1):271

Figures

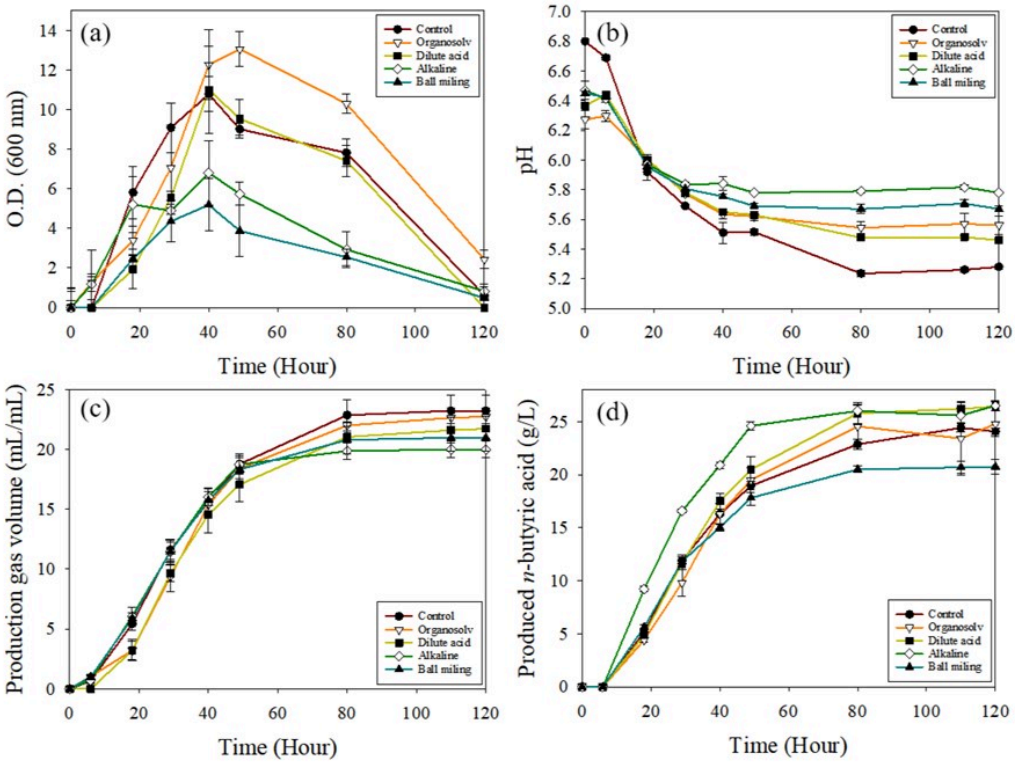


Figure 1

Fermentation profiles of *C. tyrobutyricum* BAS7 under different pretreatment conditions. The profiles depict cell growth (a), pH (b), fermentation gas volume (c), and *n*-butyric acid concentration (d) during cultivation. Data are presented as mean ± standard deviation (n = 2 for the control and n = 3 for each pretreatment condition). Filled circles represent control (●), downward open triangles indicate organosolv (▽), filled squares represent dilute acid (■), open diamonds indicate alkaline (◇), and upward filled triangles represent ball-milling conditions (▲).

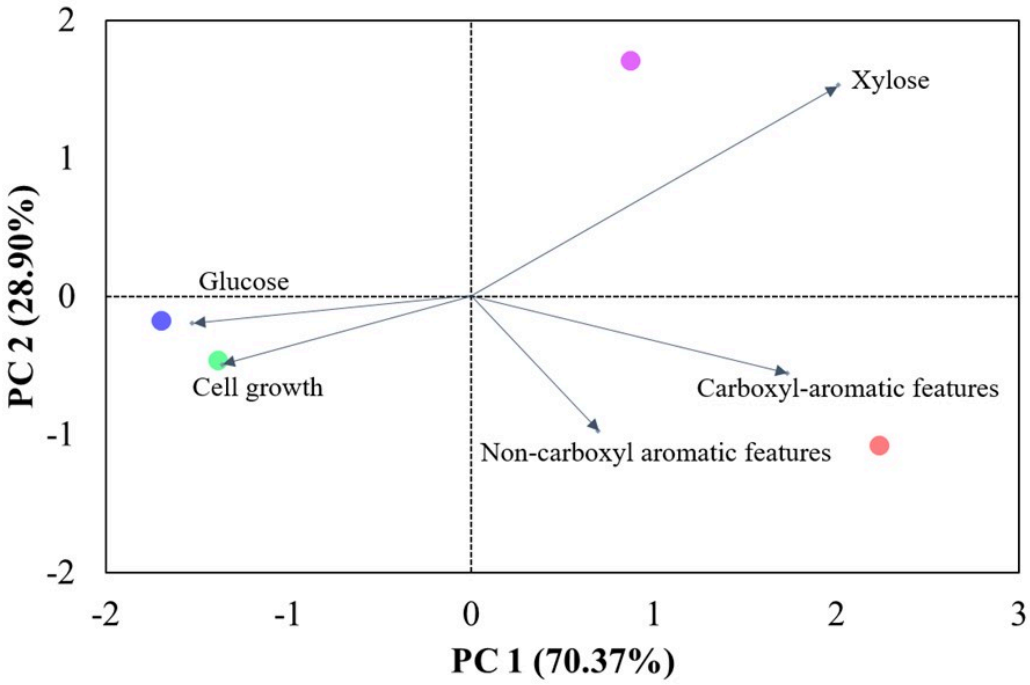


Figure 2

PCA biplot of fermentation-related variables for *C. tyrobutyricum* BAS7 cultivated with four pretreatment-derived hydrolysates. Circles represent pretreatment conditions, and arrows denote loading vectors for cell growth, glucose, xylose, and summed TIC areas of carboxyl-containing aromatic features and non-carboxyl aromatic features. The blue circle (●) represents organosolv, the green circle (●) represents dilute acid, the pink circle (●) represents ball milling, and the orange circle (●) represents alkaline. The percentages on the axis indicate the explained variance (PC1, 70.37%; PC2, 28.90%).

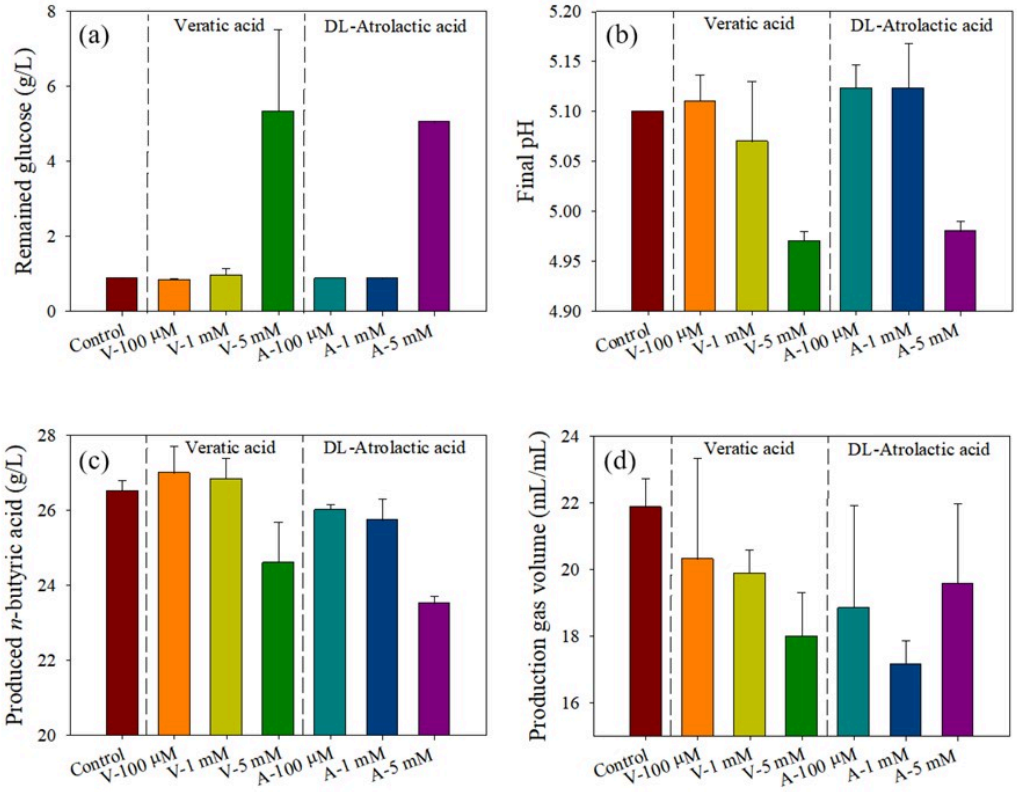


Figure 3

Fermentation results of *C. tyrobutyricum* BAS7 under different concentrations of veratric acid and DL-atrolactic acid. The bar graphs illustrate residual glucose concentration (a), final pH (b), final *n*-butyric acid concentration (c), and fermentation gas volume (d). Control (dark red), 100 μM veratric acid (orange), 1 mM veratric acid (yellow-green), 5 mM veratric acid (green), 100 μM DL-atrolactic acid (light blue), 1 mM DL-atrolactic acid (blue), and 5 mM DL-atrolactic acid (purple). Data are expressed as mean ± standard deviation (n = 3).

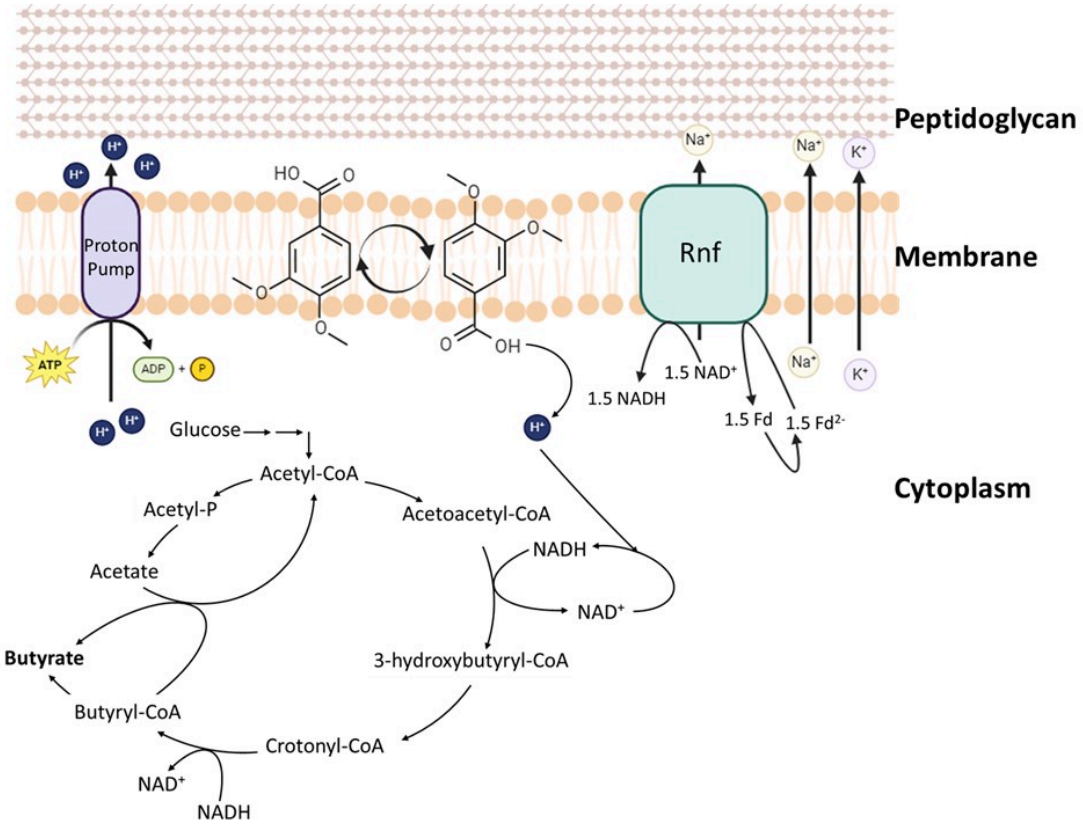


Figure 4

Working hypothesis for the possible effects of hydrolysate-derived aromatic compounds on *C. tyrrobutyricum* fermentation. Aromatic compounds may affect membrane-associated or redox-related processes, which could influence fermentation gas formation and product distribution. Dashed arrows indicate hypothetical relationships that were not directly measured in this study.

Supplementary Files

This is a list of supplementary files associated with this preprint. Click to download.

- 2.SupplementaryfileEV1HJM.docx
- GraphicalabstractFIN2.jpg